Glycoconj J (2008) 25:137–143
DOI 10.1007/s10719-007-9065-9

Interaction of a *Salmonella enteritidis* O-antigen octasaccharide with the phage P22 tailspike protein by NMR spectroscopy and docking studies

Jens Landström · Eva-Lisa Nordmark · Robert Eklund · Andrej Weintraub · Robert Seckler · Göran Widmalm

Received: 15 May 2007 / Revised: 2 July 2007 / Accepted: 6 July 2007 / Published online: 17 August 2007

Abstract The tailspike protein P22 recognizes an octasaccharide derived from the O-antigen polysaccharide of *Salmonella enteritidis* in a shallow groove and molecular docking successfully identifies this binding region on the protein surface. Analysis by 2D ^{1}H,^{1}H-T-ROESY and transferred NOESY NMR experiments indicate that the bound octasaccharide ligand has a conformation similar to that observed in solution. The results from a saturation transfer difference NMR experiment show that a large number of protons in the octasaccharide are in close contact with the protein as a result of binding. A comparison of the crystal structure of the complex and a molecular dynamics simulation of the octasaccharide with explicit water molecules suggest that only minor conformational changes are needed upon binding to the tailspike protein.

Keywords Carbohydrates · Conformation · STD · Hydrolase · Docking · Molecular dynamics

J. Landström · E.-L. Nordmark · R. Eklund · G. Widmalm (✉)
Arrhenius Laboratory, Department of Organic Chemistry,
Stockholm University, 106 91 Stockholm, Sweden
e-mail: gw@organ.su.se

A. Weintraub
Division of Clinical Microbiology,
Department of Laboratory Medicine, Karolinska Institute,
Karolinska University Hospital,
141 86 Stockholm, Sweden

R. Seckler
Physical Biochemistry, Potsdam University,
Karl-Liebknecht-Str. 24-25,
14476 Potsdam-Golm, Germany

Introduction

The polysaccharide components of bacteria have important structural and functional roles. Upon infection the bacteriophages use surface carbohydrates such as lipopolysaccharide (LPS) molecules as receptors [1]. These processes involve protein–ligand interactions and are essential in the interplay between different organisms. The *Salmonella* serogroups A, B and D_1 have a trisaccharide element, Gal-Man-Rha in the O-antigen repeating unit in common and a fourth sugar, a 3,6-dideoxyhexose residue specific to the serogroup, namely, paratose, abequose or tyvelose, respectively. The antigenic determinants or epitopes recognized by antibodies are these 3,6-dideoxyhexoses [2].

The conformation of oligosaccharides related to O-antigenic polysaccharide chains of different *Salmonella* serogroups have previously been studied using semiempirical calculations in the form of the Hard-Sphere, Exo-Anomeric Approach [3], in which the conformational preference at the ϕ torsion angles is governed by the *exo*-anomeric effect [4]. ^{1}H and ^{13}C NMR spectra of several of these oligosaccharides were also assigned [5]. The octasaccharide derived from the *Salmonella enteritidis* (previously known as Serogroup D_1) O-antigen constitutes two repeating units of the O-polysaccharide. It corresponds to a backbone repeated twice with the sequence →3)-α-D-Gal*p*-(1→2)-α-D-Man*p*-(1→4)-α-L-Rha*p*-(1→ to which tyvelose (3,6-dideoxy-D-*arabino*-hexopyranose) groups are α-(1→3)-linked to each of the mannosyl residues. We herein investigate conformational preferences of an octasaccharide derived from the serogroup D_1 LPS and its binding to the phage P22 tailspike protein (TSP), which also has hydrolyzing activity, and is part of the bacteriophage's tail machine [6].

Materials and methods

Sample preparation

The octasaccharide from the *S. enteritidis* O-antigen was prepared by depolymerization of the alkaline treated LPS with the phage P22 endorhamnosidase in a dialysis bag followed by gel permeation chromatography as previously described [7]. The tailspike protein lacking the N-terminal domain, TSPΔN, was expressed and purified as described previously [8]. The octasaccharide (7.0 mg) was lyophilized and subsequently dissolved in D_2O (0.6 ml) to give a concentration of 8 mM. The protein was freeze-dried from a stock solution buffered with sodium phosphate (100 mM, pH 7.0) containing 6 mg·ml^{-1} and subsequently dissolved, together with the octasaccharide, in an equivalent amount of D_2O (0.6 ml), giving a monomer concentration of 100 μM and an octasaccharide concentration of 1.0 mM. The resulting protein–ligand molar ratio was thus ~1:10 with respect to each of the three identical binding sites of TSPΔN.

NMR spectroscopy

The NMR experiments were carried out at 35 and 55°C on a Bruker DRX 500 MHz spectrometer equipped with a 5 mm PFG triple-resonance CryoProbe and on a Varian Inova 600 MHz spectrometer equipped with a 5 mm PFG triple-resonance probe. ^{1}H,^{1}H-NOESY, ^{1}H,^{1}H-ROESY and ^{1}H,^{1}H-T-ROESY [9] spectra were acquired at 600 MHz using a mixing times of 30–300 ms and a sweep width of 2100 Hz in both dimensions. Data were collected with 40–64 transients using 4,096 data points and 128 t_1-increments. The STD spectrum was recorded at 500 MHz with 32 dummy scans, 17 K transients and 16 K data points over a spectral width of 6510 Hz. The initial part of the experiment consisted of a relaxation delay of 2.7 s. Selective presaturation of the protein was achieved by Gaussian-shaped pulses of 50 ms duration, an irradiation power $\gamma B_1/2\pi = 76$ Hz, a delay between pulses of 1 ms and a total saturation time of 1.0 s. The on-resonance irradiation of the protein was set at a chemical shift of −0.5 ppm and the off-resonance irradiation was applied at 30 ppm. Subtraction of on- and off-resonance spectra was achieved via phase cycling. A 60-ms spin-lock pulse with a strength of $\gamma B_1/2\pi = 4.2$ kHz was applied to remove background protein signals. The HDO signal was suppressed via a WATERGATE scheme using a 3-9-19 pulse sandwich, with a delay τ=0.25 ms, bracketed by two pulsed field gradients of equal intensity and sign.

Molecular modeling

The crystal structure of the complex between the octasaccharide and the tailspike protein of *Salmonella* phage P22 was used as a starting point (1TYU) [10]. Docking of the octasaccharide to the protein was performed with the program AutoDock [11] (version 3.0) including its empirical force field, to find optimal conformations of carbohydrate-protein complexes [12]. The initial docking used a grid of 100 points in each direction with a spacing of 1.0 Å and no internal degrees of freedom for the ligand. Subsequently, finer sets of parameters were used throughout the search. The final Lamarckian Genetic algorithm docking protocol utilized as internal degrees of freedom 30 torsion angles, including 14 glycosidic torsions and hydroxyl torsions of the octasaccharide (close to the protein surface in the crystal structure), a grid size of 120 points in each direction, a spacing of 0.375 Å, a population size of 200 individuals with the maximum number of energy evaluations and generations set to 10^7 and 10^4, respectively and the mutation and cross-over rates set to 0.1 and 0.8, respectively.

Molecular dynamics (MD) simulations used NAMD [13, 14] (parallel version, 2.6 b1) employing a CHARMM22 type of force field [15], namely PARM22/SU01 [16], which is a recently modified force field for carbohydrates. Pdb and psf files of the octasaccharide, having the α-anomeric form at its reducing end, were created using VEGA [17] (release ZZ 2.0.6). Initial conditions were prepared by placing the octasaccharide in a previously equilibrated cubic water box with initial length of 50 Å. This procedure resulted in a system with the octasaccharide and 5524 TIP3P water molecules. The MD simulation was carried out with multiple-time-stepping and 2, 2, and 4 fs were used as the inner, middle and outer time steps [14]. Following equilibration of the system the production run was carried out for a 5 ns duration period performed in the NPT ensemble (P= 1 atm, T=300 K) with a cutoff distance for non-bond interactions set at 12 Å and periodic boundary conditions giving a cubic box of approximately 49 Å to the side. The smooth particle-mesh Ewald (SPME) method was used to calculate the full electrostatic interactions. The temperature and pressure were kept constant using a Langevin thermostat and a Langevin barostat, respectively. All bonds to hydrogen atoms were kept rigid. Data were saved every 500 time steps for analysis.

Results and discussion

The octasaccharide has a rhamnose residue at the reducing end (Fig. 1), leading to an anomeric mixture with two sets of resonances for this residue. The ^{1}H and ^{13}C NMR chemical shifts were similar to those reported for related molecules [5, 18], consistent with the structure of the octasaccharide. Prior to the present study it was known that the tailspike protein is quite tolerant to elevated temperatures, *i.e.*, up to at least 80°C. In order to study the bound

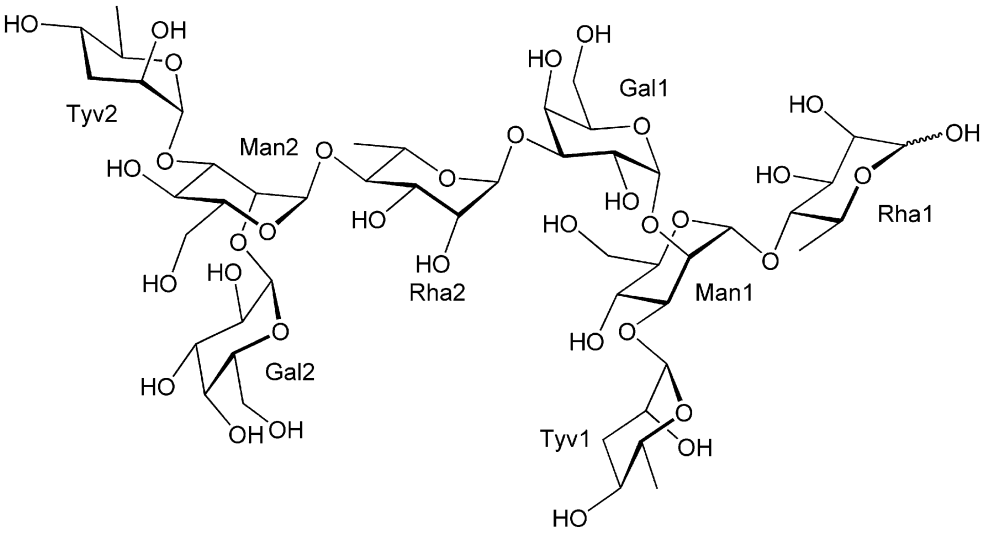

Fig. 1 Schematic of the octasaccharide derived from the *S. enteritidis* O-antigen

conformation of the octasaccharide to its receptor by transferred ^{1}H,^{1}H-NOESY experiments the off-rate (k_{off}) from the protein needs to be high enough. The dissociation rate constant for methyl β-lactoside binding to the ricin B-chain lectin was estimated to be on the order of 50 s^{-1} at 30°C [19]. The kinetics between 10 and 30°C have been investigated for the tailspike protein and the octasaccharide and the off-rate was found to be 0.25 and 3.8 s^{-1}, respectively [20]. With this in mind transferred NOESY (tr-NOESY) experiments should be performed at a higher temperature. In the above temperature range a small oligosaccharide such as a disaccharide will show a positive ^{1}H,^{1}H-NOE at a spectrometer with a ^{1}H frequency of 500–600 MHz. However, under such experimental conditions the octasaccharide will report negative NOEs, which is also the case for the ligand bound to the protein in a tr-NOESY experiment. In order to determine suitable experimental conditions one-dimensional ^{1}H,^{1}H-NOESY experiments were performed on the octasaccharide starting from 25°C, increasing the temperature by 10°C for each experiment until 55°C, where the conditions indicated that the NOE was small at 14.1 T due to the zero-crossing at $\omega\tau_c = \sqrt{5/4}$, where ω is the spectrometer frequency and τ_c is the correlation time of the molecule. At this temperature the extrapolated off-rate for the carbohydrate–protein complex is k_{off} ~80 s^{-1}. Thus, in the tr-NOESY experiments the contribution from the free ligand in solution should be negligible compared to that originating from the protein–ligand complex.

The overall conformation of the octasaccharide in solution was investigated by 2D ^{1}H,^{1}H-T-ROESY experiments. In particular, we analyzed the octasaccharide in comparison to

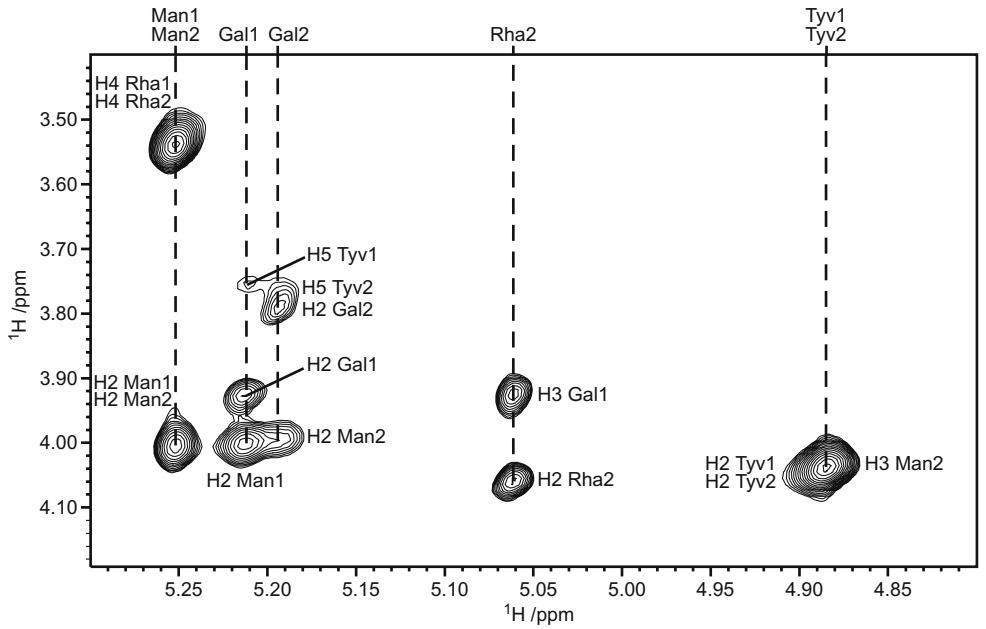

Fig. 2 A selected region of a tr-NOESY NMR spectrum of the octasaccharide in the presence of tailspike protein. A mixing time of 120 ms was used. Correlations between anomeric protons and other protons in the sugar residues are observed as cross-peaks which have been annotated

the conformation observed for a trisaccharide, α-D-Gal*p*-(1→2)[α-Abe*p*-(1→3)]-α-D-Man*p*-OMe [2], corresponding to the branching region in the O-antigen of *Salmonella typhimurium* which carries abequose groups in lieu of tyvelose groups present in the O-chain of *S. enteritidis*. The NOE between H1 in Gal and H5 in Abe in the trisaccharide was larger than between H1 in Gal and H3 in Abe, whereas in a Fab-trisaccharide complex the reverse was observed [2]. In the octasaccharide the T-ROE between H1 in Gal and H5 in Tyv was also larger than between H1 in Gal and H3 in Tyv, indicating a similar conformational preference in the two compounds and possibly in the O-chains of the corresponding serogroups. Analysis of the tr-NOESY [21–23] data (Fig. 2) indicated that the bound ligand has a conformation similar to that observed in solution.

In describing the interaction between the protein and the ligand, mapping of the binding epitope is also of great interest. This can be carried out using the STD NMR technique [24], which is based on transfer of saturation [25] from the protein to the bound ligand [26]. The ^{1}H NMR

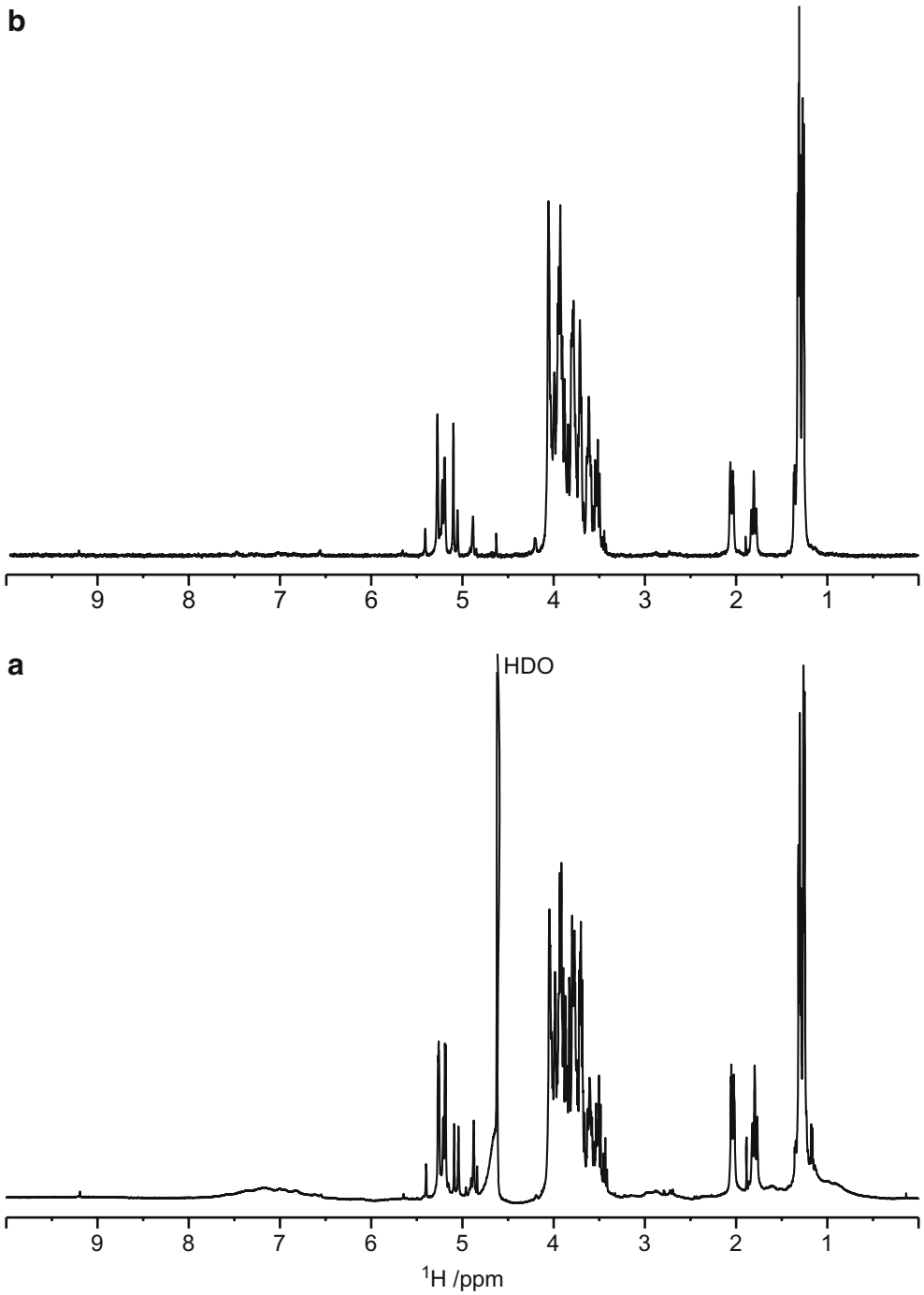

Fig. 3 **a** The ^{1}H NMR spectrum of the octasaccharide in the presence of tailspike protein; **b** The corresponding ^{1}H-STD NMR spectrum

Table 1 Glycosidic torsion angles (°) of the octasaccharide derived from the O-antigen of *S. enteritidis*

Torsion angle	Crystal structure (1TYU)	Docked conformer 1[a]	Docked conformer 2[b]	HSEA calculation[c]	MD simulation[d]
ϕ_{Tyv2}	−56	31	0	−51	−48 (9)
ψ_{Tyv2}	9	28	9	−12	5 (22)
ϕ_{Gal2}	−49	−16	−31	−44	−40 (9)
ψ_{Gal2}	28	3	10	−19	32 (25)
ϕ_{Man2}	−26	−41	−49	−36	−30 (28)
ψ_{Man2}	−7	−21	−23	−1	15 (30)
ϕ_{Rha2}	56	30	43	50	49 (10)
ψ_{Rha2}	13	−8	6	6	17 (23)
ϕ_{Tyv1}	−53	−52	−74	−51	−51 (10)
ψ_{Tyv1}	13	−15	−3	−12	2 (21)
ϕ_{Gal1}	−33	4	−35	−44	−45 (11)
ψ_{Gal1}	32	28	31	−19	12 (36)
ϕ_{Man1}	−41	−76	−29	−36	−32 (22)
ψ_{Man1}	10	−18	8	−1	16 (29)

[a] $\Delta G_{binding}$=−13.0 kcal·mol^{-1}
[b] $\Delta G_{binding}$=−12.5 kcal·mol^{-1}
[c] Torsion angles from pentasaccharide in [3].
[d] Average torsion angles from the 5 ns simulation. Root-mean-square deviation (RMSD) in parenthesis.

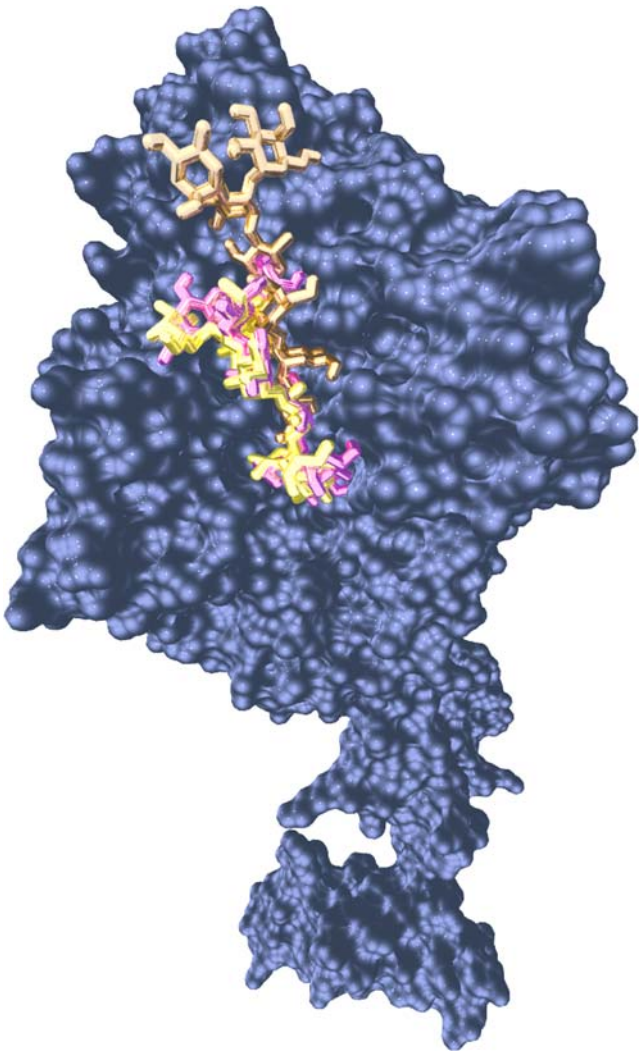

Fig. 4 Molecular model of the octasaccharide-TSP complex with the lowest intermolecular interaction energy observed upon docking (*brown*) in which the ligand is shifted away from the active hydrolysis site and the next to lowest energy (yellow) which is similar to the crystal structure of the complex (*purple*). Only one subunit of the trimeric TSP is shown

spectrum of the mixture shows narrow resonances for the octasaccharide, but from the tailspike protein, being a trimer with a molecular mass of ~180 kDa, they are broad (Fig. 3a). The ^{1}H-STD NMR spectrum of the mixture (Fig. 3b) reveals signals from anomeric protons, ring protons, the protons of the methylene groups of the tyvelose residues, and from methyl groups of both tyvelose and rhamnose residues. The STD epitope map is sensitive to differences in ^{1}H T_1 relaxation times [27]. Therefore, the proton T_1 relaxation times of the octasaccharide in D_2O solution as well as the exchange-averaged T_1 values of the ligand in the mixture were measured. The T_1 values usually became longer and less different in the mixture where we

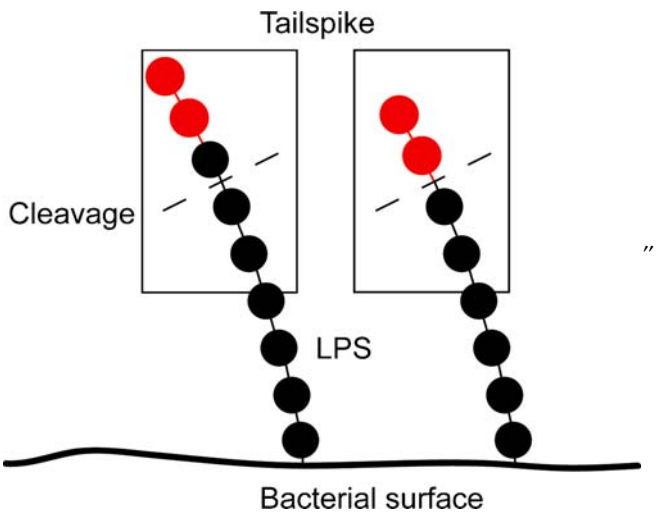

Fig. 5 Schematic representation of the binding of the TSP to the terminal part of the O-antigen polysaccharide covering two or three repeating units up to the active hydrolysis site. A *filled circle* represents one repeating unit. *Red filled circles* also represent two repeating units and indicate approximately where the octasaccharide is binding to the TSP

observed T_1 ~1 s. In the subsequent analysis we therefore utilized a relatively short saturation time of 1 s. A few conspicuous differences between the ^{1}H and the STD NMR spectra are however evident, namely, a relative increase of the signal intensity for the H1 resonance from α-Rha1 at 5.10 ppm, and relative decrease for the H1 resonance from Gal2 at 5.20 ppm as well as signals from H1 of Tyv residue(s) at 4.89 ppm. The results from the STD NMR experiment show that a large number of protons in the octasaccharide are in close contact with the protein as a result of binding. These findings indicate close proximity of H1 in α-Rha1 to the protein, whereas less contact between the protein and the terminal Gal2 residue is suggested. The relatively looser binding of at least one of the Tyv side-chain residues is not inconsistent with the fact that the TSP is able to bind to and hydrolyze different *Salmonella* O-antigens where the epitope dominant sugar is a 3,6-dideoxyhexose. In the crystal structure of the octasaccharide complex (1TYU), one of the tyveloses (the one in the reducing end O-antigen repeat) hardly interacts with the protein surface, whereas the second tyvelose residue makes intensive contacts in a surface pocket of the protein.

In order to investigate differently bound conformations a computational docking procedure was implemented [11], starting out from the crystal structure (Table 1). A grid of possible sites on the protein was sampled and the intermolecular interaction energy for each arrangement was evaluated. In the final docking protocol the lowest energy binding model (Conformer 1 in Table 1), with a binding free energy of −13.0 kcal·mol^{-1}, was a structure in which the binding mode was 'shifted by one repeating unit' towards the non-reducing end, away from the active hydrolysis site (Fig. 4). The binding model with the next to lowest binding free energy of −12.5 kcal·mol^{-1} (Conformer 2 in Table 1) showed a similar arrangement as that in the protein–ligand crystal. Taken together, these two docking models describe the interaction of 'three repeating units' and the results are consistent with the observed STD effect on H1 of α-Rha1 and the lower STD effect on H1 of Gal2, if the NMR experiment is sampling the binding of the octasaccharide to 'two sites' on the extended shallow binding groove.

The conformation of the octasaccharide bound to the protein as deduced from the crystal structure of the complex can be compared to that of the docked low energy conformers, previous HSEA calculations on related compounds and a molecular dynamics (MD) simulation of the octasaccharide with explicit water performed herein (Table 1). The docked octasaccharide conformer 2, which is positioned like in the crystal structure, has indeed a similar conformation as the octasaccharide in the crystal structure 1TYU. Only the ϕ_{Tyv2} torsion angle of the terminal tyvelose residue shows a significant deviation. The average deviation of the torsion angles is defined by $\Delta_{octa} = \frac{1}{n}\sum_{i}^{n} |\theta_i(\text{structure}) - \theta_i(\text{crystal})|$ where $\theta=\phi$ or ψ and $n=14$. For conformer 2 $\Delta_{octa}=15°$. Also for the docked conformer 1 the largest deviation is observed for ϕ_{Tyv2} to a non-*exo*-anomeric conformation, which is possible due to the axial hydroxyl group at C2 in the tyvelose group. For this octasaccharide conformation $\Delta_{octa}=27°$. For comparison to the HSEA-derived models, pentasaccharide data [5] were used to approximate the present octasaccharide. One then obtains $\Delta_{octa}=15°$ for the HSEA model, *i.e.*, on the same order of magnitude as for the docked conformer 2 that is positioned as in the crystal structure. To estimate the conformational dynamics of the octasaccharide in solution a 5 ns MD simulation [13, 14] was performed using a recently developed force field for carbohydrates [16]. The ϕ torsion angles populate mainly the conformational space governed by the *exo*-anomeric effect with RMSD values of ~10°. The ψ torsion angles are slightly positive with RMSD-values of ~30° and conformational transitions between states do occur during the time scale of the simulation. Although the oligosaccharide populates several conformational states during the simulation a comparison to the crystal structure gives $\Delta_{octa}=9°$ for the MD-derived data. The latter indicates that only minor changes are needed upon binding to the tailspike protein and these may be induced by the protein or just adapted as part of the dynamic processes in the polysaccharide.

The two major products from cleavage of the O-antigen by the TSP are octa- and dodecasaccharides, *i.e.*, two and three repeating units. Thus, the binding observed for the octasaccharide in this study is complex but consistent with a model in which the phage with its TSP binds to and cleaves the terminal part of the O-antigen chain (Fig. 5). Notably, fluorescence and calorimetry data indicate that binding affinities and dissociation kinetics are essentially identical for the octasaccharide studied here and for the dodecasaccharide comprising three repeats of the O-antigen [8, 20]. NMR studies with the dodecasaccharide and non-hydrolyzing mutants, which are available, would be very interesting in order to elucidate the binding process in greater detail.

Acknowledgements This work was supported by grants from the Swedish Research Council (VR), the Swedish Foundation for Strategic Research (GLIBS), the Swedish National Infrastructure for Computing (SNIC) and the German Science Foundation (DFG).

References

1. Steinbacher S., Miller S., Baxa U., Budisa N., Weintraub A., Seckler R., Huber R.: Phage P22 tailspike protein: Crystal structure of the head-binding domain at 2.3 Å, fully refined structure of the endorhamnosidase at 1.56 Å resolution, and the molecular basis of the O-antigen recognition and cleavage. J. Mol. Biol. **267**, 865–880 (1997)

2. Bundle D.R., Baumann H., Brisson J.-R., Gagné S.M., Zdanov A., Cygler M.: Solution structure of a trisaccharide–antibody complex: Comparison of NMR measurements with a crystal structure. Biochemistry **33**, 5183–5192 (1994)
3. Bock K., Meldal M., Bundle D.R., Iversen T., Garegg P.J., Norberg T., Lindberg A.A., Svenson S.: The conformation of *Salmonella* O-antigenic polysaccharide chains of serogroups A, B, and D_1 predicted by semi-empirical, hard-sphere (HSEA) calculations. Carbohydr. Res. **130**, 23–34 (1984)
4. Lemieux R.U., Koto S.: The conformational properties of glycosidic linkages. Tetrahedron **30**, 1933–1944 (1974)
5. Bock K., Meldal M., Bundle D.R., Iversen T., Pinto B.M., Garegg P.J., Kvarnström I., Norberg T., Lindberg A.A., Svenson S.: The conformation of *Salmonella* O-antigenic oligosaccharides of serogroups A, B, and D_1 inferred from ^{1}H- and ^{13}C-nuclear magnetic resonance spectroscopy. Carbohydr. Res. **130**, 35–53 (1984)
6. Tang L., Marion W.R., Cingolani G., Prevelige Jr P.E., Johnson J. E.: Three-dimensional structure of the bacteriophage P22 tail machine. EMBO J. **24**, 2087–2095 (2005)
7. Eriksson U., Svenson S.B., Lönngren J., Lindberg A.A.: *Salmonella* phage glycanases: Substrate specificity of the phage P22 endo-rhamnosidase. J. Gen. Virol. **43**, 503–511 (1979)
8. Baxa U., Steinbacher S., Miller S., Weintraub A., Huber R., Seckler R.: Interactions of phage P22 tails with their cellular receptor, *Salmonella* O-antigen polysaccharide. Biophys. J. **71**, 2040–2048 (1996)
9. Hwang T.-L., Kadkhodaei M., Mohebbi A., Shaka A.J.: Coherent and incoherent magnetization transfer in the rotating frame. Magn. Reson. Chem. **30**, S24–S34 (1992).
10. Steinbacher S., Baxa U., Miller S., Weintraub A., Seckler R., Huber R.: Crystal structure of phage P22 tailspike protein complexed with *Salmonella* sp. O-antigen receptors. Proc. Natl. Acad. Sci. U S A **93**, 10584–10588 (1996)
11. Morris G.M., Goodsell D.S., Halliday R.S., Huey R., Hart W.E., Belew R.K., Olson A.J.: Automated docking using a Lamarckian genetic algorithm and an empirical binding free energy function. J. Comput. Chem. **19**, 1639–1662 (1998).
12. Eklund R.: Computational analysis of carbohydrates: Dynamical properties and interactions. Doctoral thesis, Stockholm University, Sweden (2005).
13. Kalé L., Skeel R., Bhandarkar M., Brunner R., Gursoy A., Krawetz N., Phillips J., Shinozaki A., Varadarajan K., Schulten K.: NAMD2: Greater scalability for parallel molecular dynamics. J. Comput. Phys. **151**, 283–312 (1999).
14. Phillips J.C., Braun R., Wang W., Gumbart J., Tajkhorshid E., Villa E., Chipot C., Skeel R.D., Kalé L., Schulten K.: Scalable molecular dynamics with NAMD. J. Comput. Chem. **26**, 1781–1802 (2005)
15. MacKerell Jr A.D., Bashford D., Bellott M., Dunbrack Jr R.L., Evanseck J.D., Field M.J., Fischer S., Gao J., Guo H., Ha S., Joseph-McCarthy D., Kushnir L., Kuczera K., Lau F.T.K., Mattos C., Michnick S., Ngo T., Nguyen T.D., Prodhom B., Reiher III W. E., Roux B., Schlenkrich M., Smith J.C., Stote R., Straub J., Watanabe M., Wiórkiewicz-Kuczera J., Yin D., Karplus M.: All-atom empirical potential for molecular modeling and dynamics studies of proteins. J. Phys. Chem. B. **102**, 3586–3616 (1998)
16. Eklund R., Widmalm G.: Molecular dynamics simulations of an oligosaccharide using a force field modified for carbohydrates. Carbohydr. Res. **338**, 393–398 (2003)
17. Pedretti A., Villa L., Vistoli G.: VEGA: a versatile program to convert, handle and visualize molecular structure on Windows-based PCs. J. Mol. Graph Model. **21**, 47–49 (2002).
18. Snyder D.S., Gibson D., Heiss C., Kay W., Azadi P.: Structure of a capsular polysaccharide isolated from *Salmonella enteritidis*. Carbohydr. Res. **341**, 2388–2397 (2006).
19. Bevilacqua V.L., Thomson D.S., Prestegard J.H.: Conformation of a methyl β-lactoside bound to the ricin B-chain: Interpretation of transferred nuclear Overhauser effects facilitated by spin simulation and selective deuteration. Biochemistry **29**, 5529–5537 (1990)
20. Baxa U., Cooper A., Weintraub A., Pfeil W., Seckler R.: Enthalpic barrier to the hydrophobic binding of oligosaccharides to phage P22 tailspike protein. Biochemistry **40**, 5144–5150 (2001)
21. Clore G.M., Gronenborn A.M.: Theory and applications of the transferred nuclear Overhauser effect to the study of the conformations of small ligands bound to proteins. J. Magn. Reson. **48**, 402–417 (1982)
22. Jackson P.L., Moseley H.N.B., Krishna N.R.: Relative effects of protein-mediated spin-diffusion pathways on transferred NOESY, and implications on the accuracy of the bound ligand conformation. J. Magn. Reson. Ser. B. **107**, 289–292 (1995).
23. Poveda A., Jiménez-Barbero J.: NMR studies of carbohydrate–protein interactions in solution. Chem. Soc. Rev. **27**, 133–143 (1998)
24. Meyer B., Peters T.: NMR spectroscopic techniques for screening and identifying ligand binding to protein receptors. Angew. Chem. Int. Ed. **42**, 864–890 (2003)
25. Forsén S., Hoffman R.A.: Study of moderately rapid chemical exchange by means of nuclear magnetic double resonance. J. Chem. Phys. **39**, 2892–2901 (1963)
26. Balaram P., Bothner-By A.A., Dadok J.: Negative nuclear Overhauser effects as probes of macromolecular structure. J. Am. Chem. Soc. **94**, 4015–4017 (1972).
27. Yan J., Kline A.D., Mo H., Shapiro M.J., Zartler E.R.: The effect of relaxation on the epitope mapping by saturation transfer difference NMR. J. Magn. Reson. **163**, 270–276 (2003)